

Supporting Information

Color Stable White Organic Light-Emitting Diodes Utilizing a Blue-Emitting Electron-Transport Layer

Hao Xin,^{1,2,*} Weibo Yan,¹ Samson A. Jenekhe^{2,*}

¹*Key Laboratory for Organic Electronics and Information Displays & Jiangsu Key Laboratory for Biosensors, Institute of Advanced Materials (IAM), Jiangsu National Synergetic Innovation Center for Advanced Materials (SICAM), Nanjing University of Posts & Telecommunications, 9 Wenyuan Road, Nanjing 210023, China.*

²*Department of Chemical Engineering and Department of Chemistry, University of Washington, Seattle, Washington 98195-1750*

Email: jenekhe@u.washington.edu, iamhxin@njupt.edu.cn

Device fabrication and characterization: The ITO substrates were subsequently cleaned by acetone, ionized water, and isopropanol under sonication and dried in a 60 °C vacuum oven. The poly(ethylenedioxythiophene) : poly(styrene sulfonate) blend (PEDOT:PSS) buffer layer were spin coated on the cleaned ITO substrate from aqueous solution and annealed at 150 °C for 15 min in a vacuum furnace. The polymer blend of PVK:PBD:Ir(ppy)₃:Ir(piq)₂(acac) was then spin coated on top of PEDOT:PSS from a toluene solution and dried in a 60 °C vacuum oven over night. B2PPQ and the LiF/Al cathode were deposited by thermal evaporation under high vacuum. After the deposition of B2PPQ, the evaporation chamber was vented with air to load the cathode materials and mask the substrates and then pumped down for the deposition of LiF and aluminum. The active area of the device was 0.2 cm². The current-voltage characteristics were measured by using a HP4155A semiconductor parameter analyzer (Yokogawa Hewlett-Packard, Tokyo) and the luminance was simultaneously measured by using a model 370 optometer (UDT Instruments, Baltimore, MD) equipped with a calibrated luminance sensor head (Model 211) and a 5 × objective lens. EL spectra were obtained using a PTI QM-2001-4 spectrophotometer. All measurements were carried out under ambient air at room temperature.

Performance comparison of device A to device D.

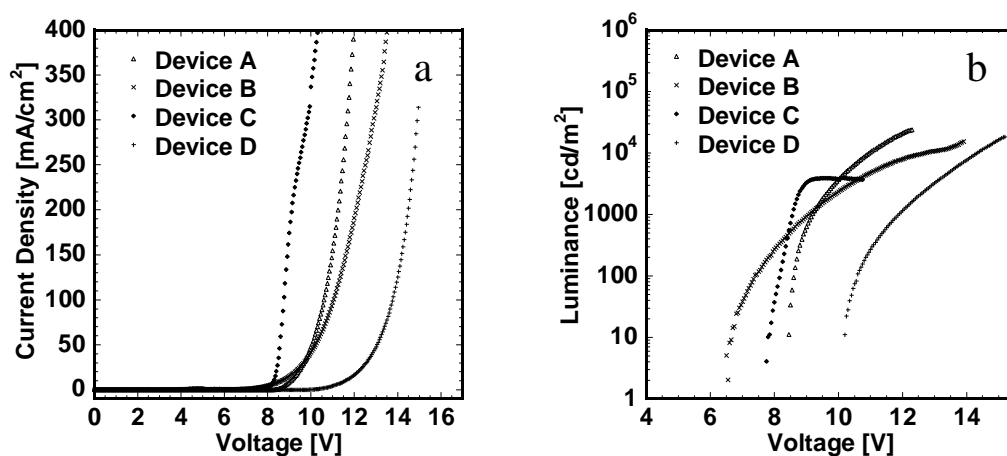


Figure S1. Comparison of current density-voltage (a) and efficiency-voltage (b) characteristics of device A: ITO/PEDOT(40 nm)/PVK:PBD:Ir(ppy)₃:Ir(piq)₂(acac)(69.1:30:0.29:0.60)(55 nm)/B2PPQ(20 nm)/LiF (1 nm)/Al, device B: ITO/PEDOT(40 nm)/PVK:PBD:Ir(ppy)₃:Ir(piq)₂(acac)(69.1:30:0.29:0.60)(75 nm)/ LiF(1 nm)/Al, device C: ITO/PEDOT(40 nm)/PVK:PBD(69.1:30)(55 nm)/B2PPQ(20 nm)/LiF(1 nm)/Al, and device D: ITO/PEDOT(40 nm)/PVK:PBD:Ir(ppy)₃:Ir(piq)₂(acac)(69.1:30:0.29:0.60)(55 nm)/B2PPQ (20 nm)/BCP(20 nm)/LiF(1 nm)/Al.

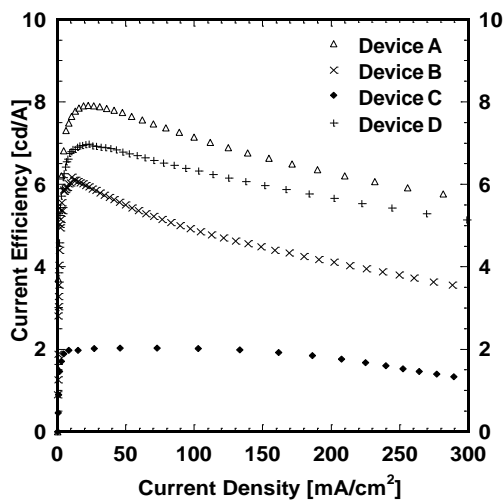


Figure S2. Comparison of luminous efficiency-current density curves of device A: ITO/PEDOT(40 nm)/PVK:PBD:Ir(ppy)₃:Ir(piq)₂(acac)(69.1:30:0.29:0.60)(55 nm)/B2PPQ(20 nm)/LiF (1 nm)/Al, device B: ITO/PEDOT(40 nm)/PVK:PBD:Ir(ppy)₃:Ir(piq)₂(acac)(69.1:30:0.29:0.60)(75 nm)/ LiF(1 nm)/Al, device C: ITO/PEDOT(40 nm)/PVK:PBD (69.1:30)(55 nm)/B2PPQ(20 nm)/LiF(1 nm)/Al, and device D: ITO/PEDOT(40 nm)/PVK:PBD:Ir(ppy)₃:Ir(piq)₂(acac)(69.1:30:0.29:0.60)(55 nm)/B2PPQ(20 nm)/BCP (20 nm)/LiF(1 nm)/Al.